DOE/NASA/50194-39
NASA TM-83627
TR-84-C-7

Cold-Air Performance of Compressor-Drive Turbine of Department of Energy Upgraded Automobile Gas Turbine Engine

III—Performance of Redesigned Turbine

Richard J. Roelke
National Aeronautics and Space Administration
Lewis Research Center

and

Jeffrey E. Haas
Propulsion Laboratory
AVSCOM Research and Technology Laboratories
Lewis Research Center

May 1984

Prepared for
U.S. DEPARTMENT OF ENERGY
Conservation and Renewable Energy
Office of Vehicle and Engine R&D

DISPLAY 35/2/1

84N25644*# ISSUE 16 PAGE 2438 CATEGORY 2 RPT#: NASA-TM-83627 E-2044 DOE/NASA/50194-39 NAS 1.15:83627 USAAVSCOM-TR-84-C-7 CNT#: DE-AI01-80CS-50194 84/01/00 40 PAGES UNCLASSIFIED DOCUMENT

UTTL: Cold-air performance of compressor-drive turbine of department of energy upgraded automobile gas turbine engine. 3: Performance of redesigned turbine

AUTH: A/ROELKE, R. J.; B/HAAS, J. E.

CORP: National Aeronautics and Space Administration, Washington, D. C.; Army Research and Technology Labs., Cleveland, Ohio. AVAIL.NTIS SAP: HC A03/MF A01

DOE/NASA/50194-39
NASA TM-83627
TR-84-C-7

Cold-Air Performance of Compressor-Drive Turbine of Department of Energy Upgraded Automobile Gas Turbine Engine

III—Performance of Redesigned Turbine

Richard J. Roelke
National Aeronautics and Space Administration
Lewis Research Center
Cleveland, Ohio 44135

and

Jeffrey E. Haas
Propulsion Laboratory
AVSCOM Research and Technology Laboratories
Lewis Research Center
Cleveland, Ohio 44135

May 1984

Work performed for
U.S. DEPARTMENT OF ENERGY
Conservation and Renewable Energy
Office of Vehicle and Engine R&D
Washington, D.C. 20545
Under Interagency Agreement DE-AI01-80C550194

COLD-AIR PERFORMANCE OF COMPRESSOR-DRIVE TURBINE OF DEPARTMENT OF ENERGY UPGRADED AUTOMOBILE GAS TURBINE ENGINE

III - Performance of Redesigned Turbine

by Richard J. Roelke
National Aeronautics and Space Administration
Lewis Research Center
Cleveland, Ohio 44135

and

Jeffrey E. Haas
U. S. Army Research and Technology Laboratory
Lewis Research Center
Cleveland, Ohio

SUMMARY

The aerodynamic performance of a redesigned compressor-drive turbine of the Department of Energy Upgraded Gas Turbine engine was determined in air at nominal inlet conditions of 325 K and 0.8 bar. Compared to the first turbine design the subject turbine had a lower flow factor, higher rotor reaction, and a redesigned inlet manifold. Two versions of the same rotor were tested: an as-cast rotor and the same rotor with reduced surface roughness. Tests were also made to determine the effect of Reynolds number on the turbine performance.

The measured turbine efficiency values at design speed and work were 0.854 and 0.859 for the as-cast and reduced roughness rotors, respectively. These efficiencies were obtained with a rotor tip clearance of 1.2 percent. At the design clearance of 2.0 percent a decrease in turbine efficiency of 0.018 was calculated, resulting in efficiencies of 0.836 and 0.841 for the two rotors. The design efficiency goal was 0.85.

At equal rotor tip clearances and design point operation the efficiency of the redesigned turbine increased 0.023 compared to the original design. An analysis of the two turbines indicated that the primary reason for the performance improvement of the redesigned turbine was lower rotor losses. There was no change in efficiency of the redesigned turbine for the range of Reynolds number covered.

INTRODUCTION

The Department of Energy (DOE) sponsored an engine research program to design, build, and test an Upgraded Gas Turbine (UGT) automotive engine. The objective was to demonstrate an updated technology gas turbine engine with fuel economy equal to or better than a conventional reciprocating engine and having low emissions. The Chrysler Corporation was awarded the DOE engine contract and the NASA Lewis Research Center agreed to technically manage the contract. A general description of the UGT engine is given in reference 1.

The Lewis Research Center also agreed to provide the initial aerodynamic designs of the compressor, compressor-drive turbine, and power turbine, as well as conduct the performance tests of these components. This report is the last in a series pertaining to the aerodynamic performance of the compressor-drive turbine.

Two compressor-drive turbines were designed and built for the UGT engine. The first was designed at Lewis and is described in reference 2. For reasons of engine packaging, casting fabrication, and engine acceleration time, several design constraints were imposed by Chrysler on this first design. The constraints that most affected the aerodynamic performance were the mandating of a single-stage axial-flow design having a work factor (i.e., $\Delta h/Um^2$) of 2.1, to minimize the polar moment of inertia; a relatively thick blade trailing edge for casting purposes; a higher than optimum flow factor (i.e., V_x/U_m) to lower blade stress; and a lower than optimum rotor reaction to minimize the exit swirl.

Stator inlet and exit surveys of this initial design (ref. 3), indicated that the flow characteristics deviated significantly from the design intent. In particular, there were thick inlet boundary layers and high incidence angles at the endwalls resulting in large losses at the stator hub and tip. Concurrent engine tests made at the Chrysler Corporation (ref. 4), indicated that the compressor-drive turbine was not meeting its performance goals at all engine speeds tested. Later engine tests made at Lewis (ref. 5), indicated that the compressor-drive turbine approached its performance goal at 95 percent design speed but fell short at lower speeds. It was left to the component stage tests to obtain a more definitive assessment of the turbine performance.

The initial stage test of this turbine, reference 6, showed an efficiency at design speed and work of only 0.78 compared to the design efficiency of 0.85. Although subsequent component testing (ref. 7), demonstrated a stage efficiency of 0.825 after reworking the blade profiles to correct casting inaccuracies, the initial indication of poor performance and consideration of project schedules resulted in a decision to design a second turbine. This turbine was designed by Chrysler utilizing the initial test results of the first design and with Pratt & Whitney/Canada acting as a consultant.

For this design some of the constraints placed on the first design were relaxed. The new design had increased rotor reaction, a lower flow coefficient, at the expense of increased blade stress, and a redesigned inlet manifold. The turbine was also designed with a nonuniform radial work distribution and a contoured stator shroud. The aerodynamic design of this turbine is briefly described in reference 4 and additional details are included herein. The experimental cold-air evaluation and analysis of the results of this turbine is the subject of this report.

The turbine blading used in the component performance tests consisted of as-cast hardware representative of the stator and rotor castings used in the engines. Because of the relatively rough surface finish of the as-cast blading, a second test was made with reduced rotor blade surface roughness. The stator was not modified. The as-cast turbine was also tested over a range of inlet total pressures to evaluate Reynolds number effects.

The performance of the turbine at its engine Reynolds number was determined with air at a nominal-inlet temperature of 325 K and an inlet pressure of 0.8 bar absolute. Performance data were taken at total-to-total pressure ratios from 1.4 to 2.4 and rotative speeds from 50 to 110 percent of equivalent design speed. Stator inlet surveys of total pressure and flow angle were taken at three stator pressure ratios and rotor exit radial surveys of total pressure, total temperature, and flow angle were made at equivalent design speed and design work factor. For the Reynolds number tests the inlet pressure was varied from 0.4 to 1.6 bars absolute, resulting in Reynolds numbers, based on mean blade radius from 1.2×10^5 to 4.8×10^5.

The aerodynamic performance of the compressor-drive turbine is presented in terms of equivalent mass flow, torque, specific work, efficiency, and flow surveys. A comparison is made between the performance of this turbine and the initially designed turbine.

SYMBOLS

AR	blade aspect ratio based on actual mean chord length and exit blade height
c	actual chord, cm
c_p	heat capacity at constant pressure, J/(kg)(K)
$\overline{e}_R$	rotor kinetic energy loss coefficient, $1 - W^2_{6.3}/W^2_{6.3,id}$
$\overline{e}_S$	stator kinetic energy loss coefficient, $1 - V^2_{5.5}/V^2_{5.5,id}$
Δh	specific work, J/kg
m	mass flow rate, kg/sec
Δm	incremental mass flow rate, kg/sec
p	absolute pressure, bars
Re	Reynolds number, $m/\mu r_m$
R_x	rotor reaction, $(P_{5.5} - P_{6.3})/(P_{4.5} - P_{6.3})$
r	radius, cm
s	blade spacing, cm
T	absolute temperature, K
U	blade velocity, m/sec
V	absolute gas velocity, m/sec
ΔV_u	change in absolute tangential velocity, m/sec
W	relative gas velocity, m/sec
WF	work factor, $\Delta h/U^2_m$
α	absolute gas flow angle measured from axial direction, deg
β	relative gas flow angle measured from axial direction, deg
γ	ratio of specific heats

δ	ratio of inlet total pressure to U. S. standard sea-level pressure, $P'_{4.5}/p^*$
ϵ	function of γ used in relating parameters to those using air inlet conditions at U. S. standard sea-level conditions, $(0.740/\gamma)\ [(\gamma+1)/2]^{\gamma/(\gamma-1)}$
η'	efficiency based on total pressure ratio $P'_{4.5}/P'_{6.3}$
$\Delta\eta'_{stage}$	loss in stage total efficiency
θ_{cr}	squared ratio of critical velocity at turbine-inlet temperature to critical velocity at U. S. standard sea-level temperature, $(V_{cr}/V^*_{cr})^2$
μ	viscosity, kg/m sec
ϕ	flow factor, V_x/U_m
τ	torque, Nm
ψ	mass flow parameter used in equation (4)

Subscripts:

av	average
cr	condition corresponding to Mach 1
id	ideal
local	local condition
m	mean
meas	measured
sur	survey
T	total
x	axial direction
4.5	station at manifold inlet (fig. 1)
5	station at stator inlet (fig. 1)
5.5	station at stator exit (fig. 1)
6.3	station at rotor exit (fig. 1)

Superscripts:

'	absolute total state
"	relative total state
*	U. S. standard sea-level conditions (temperature, 288.15 K; pressure 1.013 bars)

TURBINE DESIGN

The second design of the UGT compressor-drive turbine was a single-stage axial-flow machine with a rotor tip diameter of 11.46 cm. The inlet manifold was a spiral-shaped volute with a single entry. The stator had a contoured outer wall with a vane height of 1.65 cm at the leading edge and 1.28 cm at the trailing edge. The blades of this turbine were 15 percent longer than the first turbine design. A cross-section of the turbine as it appeared in the test rig is shown in figure 1. The instrumentation stations shown in figure 1 are further defined in the section RESEARCH EQUIPMENT AND PROCEDURES. The duplicate engine parts used in the test rig were the inlet volute, the stator ring, and the rotor. Photos of these parts are shown in figure 2.

The hot engine, equivalent design and nominal component test conditions are listed in table I. The turbine hardware was fabricated slightly undersize so that the flow passage would expand to the design area when the engine was operating at the design inlet temperature. Thus, it is necessary to show the equivalent flow conditions for both hot and cold hardware. The inlet temperature during the component test (table I), was selected to avoid exhaust duct icing and the inlet pressure was set to replicate the hot turbine Reynolds number.

The turbine design velocity diagrams are shown in figure 3. The radial gradients of pressure and tangential momentum used to generate these diagrams were based on the survey data obtained with the first inlet volute. Comparison of these diagrams to those of the first turbine design (ref. 2), shows that the second design had lower stator velocities, higher rotor reaction, and increased exit swirl. Specifically, at the mean radius, the second turbine design had a stator exit velocity ratio of 0.847 versus 0.929, a rotor reaction, R_x, of 0.357 versus 0.258, and an exit swirl of 30.9° versus 21.1°. The design radial variation of work is shown in figure 4. As the figure shows the specific work was greatest at the mid-span and reduced at the endwalls.

The redesigned inlet manifold is a single entry volute, as was the first manifold, but with much larger volume and without the axisymmetric chute at the stator inlet. The calculated velocities in the redesigned volute were about 30 percent lower than the original volute. The axisymmetric chute of the first design was replaced by a highly converging section at the stator inlet. These changes in the volute design were made to reduce the turbine inlet wall boundary layers which were as thick as 20 percent of the passage in the first design.

The stator and rotor profiles are shown in figure 5. The stator had 15 vanes, an aspect ratio of 0.43 (based on the exit blade height), and a contoured shroud wall. Table II lists further design parameters. Major geometric differences between this stator and the first stator design are: nominally 30 percent higher solidity, exit angles 6° to 7° nearer tangential in the mean and tip regions, and design incidence angles 9 to 15 degrees higher at the hub and tip, respectively.

The design parameters for the rotor are listed in table III. The solidity of this design was nominally 8 percent higher than the first design and had 8° to 14° more turning at the hub and mean sections, respectively. The design rotor tip clearance was the same for both turbines (0.25 mm) but due to the

longer blade of the second design, the blade clearance, as a percentage of the blade height, was slightly reduced, from 2.2 to 2.0. In the component performance tests, the tip clearances were nominally 1.7 and 1.2 percent of the rotor blade height for the first and second designs, respectively. Comparisons of design parameters of the two turbines are summarized in table IV.

The design stator and rotor blade surface velocities are shown in figures 6 and 7. The calculation was made by Chrysler using the computer code described in reference 8. A second calculation of the blade surface velocities was recently made to assist in analyzing the measured turbine performance. The results of that computation are given in the section labeled Analytical Results.

RESEARCH EQUIPMENT AND PROCEDURE

The apparatus used in this investigation consisted of the research turbine, an airbrake dynamometer used to control the speed and absorb and measure the power output of the turbine, an inlet and exhaust piping system including flow controls, and appropriate instrumentation. Figure 8 shows a schematic of the facility and a photograph of the test installation. The rotational speed of the turbine was measured with an electronic counter in conjunction with a magnetic pickup and a shaft-mounted gear. Mass flow was measured with a calibrated venturi. Turbine torque was determined by measuring the reaction torque of the airbrake, which was mounted on air trunnion bearings, and adding corrections for the turbine bearings and seal losses and the coupling and rotor disk windage loss. These tare losses were previously measured and corresponded to about 7.5 percent of the measured torque obtained at design equivalent speed and work factor. The torque was measured with a commercial strain-gage load cell.

The turbine instrumentation stations are shown in figure 1. Figure 9 shows the instrumentation at each station. Stations 4.5 and 5 were chosen because they corresponded to the station locations in the UGT test engine (ref. 4). Stations 5.5 and 6.3 were added for component testing. Instrumentation at the manifold inlet (station 4.5) measured wall static pressure, total pressure, and total temperature. At the stator inlet (station 5), located approximately 0.60 centimeter upstream of the stator, the static pressure, total pressure,and flow angle were measured. Static pressures were obtained from six taps, with three each on the inner and outer walls. The inner and outer wall taps were located opposite each other at different intervals around the circumference. Two radial traversing probes, located midway between adjacent stator vanes, were used to determine the radial variation in total pressure and flow angle. These probes were positioned at a fixed angle, and the total pressure and flow angle were determined from calibration curves. At the stator exit (station 5.5) located 1 mm downstream of the stator trailing edge, static pressures were measured with six taps, with three each on the inner and outer walls, located opposite each other at different intervals around the circumference.

At the rotor exit (station 6.3), located about three axial chord lengths downstream of the rotor, static pressure, total pressure, total temperature, and flow angle were measured. The static pressure was measured with six taps,

with three each on the inner and outer walls. Three self-aligning radial-traversing probes located around the circumference were used for measurement of total pressure, total temperature, and flow angle. Station 6.3 was located downstream of the rotor where the rotor blade wakes were uniformly mixed-out.

The stage test program consisted of three parts: Part I determined the turbine performance with the as-cast blading over a range of equivalent total pressure ratios and rotative speeds. The manifold-inlet-total to rotor-exit-total pressure ratio was varied from 1.4 to 2.4 and the speed from 50 to 110 percent of equivalent design speed. Part II was a Reynolds number evaluation of the as-cast blading. Reynolds number was varied from 1.2×10^5 to 4.8×10^5 over a range of turbine pressure ratios at design equivalent speed. Reynolds number was changed by varying the turbine inlet pressure from 0.4 to 1.6 bars absolute. The third part of the stage test program determined the turbine performance with reduced rotor blade surface roughness. The blade surface finish was smoothed in the same manner as the first turbine. The suction surface was hand-polished and a coat of lacquer was applied to the pressure surface. Table V lists the rotor surface finishes of both turbines before and after smoothing. The particular geometry of the integrally cast stator prevented measuring and smoothing the vane surface finish. The appearance of the surface finish of the as-cast stator was similar to the as-cast rotor.

In each part of the test progam, a rotor-exit radial survey was first conducted at equivalent design values of speed and specific work. Radially mass-averaged values of flow angle, total temperature, and total pressure were obtained for each of the three circumferential survey locations at station 6.3. These mass-averaged values were then arithmetically averaged to obtain overall values. The survey probes were then positioned with one each near the tip, near midspan, and near the hub so that the average flow angle from these three positions would correspond closely to the overall mass-averaged value obtained from the survey. Performance data were then obtained at other operating conditions.

The stage evaluation was conducted in air at nominal inlet conditions of 326 K and a range of turbine-inlet pressures from 0.4 to 1.6 bars absolute. The turbine was rated on the basis of total efficiency. The actual work was calculated from torque, speed, and mass flow measurements. The ideal work was based on the manifold-inlet-to-rotor-exit total pressure ratio. The manifold-inlet (station 4.5) and rotor-exit (station 6.3) total pressures were calculated from mass flow, static pressure, total temperature, and flow angle. For the calculation of manifold-inlet total pressure the flow angle was assumed to be zero.

ANALYSIS METHOD

In order to make a more detailed assessment of the efficiency improvement of the second turbine compared to the first turbine, detailed loss analyses were made for both turbines. The procedure, described fully in reference 9, analytically calculates the turbine losses for a given turbine geometry, turbine operating condition, and flow field at the stator inlet. For each turbine the stator and rotor coordinates were adjusted based on throat measurements to reflect the actual test hardware. The analyses were made at

two operating conditions: at design equivalent speed and work, and at 70 percent of design equivalent speed and a stage pressure ratio of 1.45. This latter condition corresponds to a part power condition where the turbine operates a major part of the time when installed in the engine. The stator inlet flow characteristics of endwall displacement thicknesses, flow angle radial distributions and volute total pressure losses were obtained using experimental results from the two turbine tests. The measured stator pressure ratio was also specified for the calculation. The procedure followed used the MERIDL and TSONIC computer codes (refs. 8 and 10), to compute flow conditions in the blade channels including blade surface and endwall velocities. The BLAYER computer code (ref. 11), was then used to calculate stator and rotor displacement and momentum thicknessess, which were, in turn, used to calculate profile friction losses (including the mixing loss) and endwall friction losses. Additional published correlations were used to calculate losses due to incidence, secondary flow, rotor tip clearance, and the exhaust duct friction. Losses were calculated as kinetic energy loss coefficients ($\bar{e}$) for the stator and rotor. For each blade row, the total kinetic energy loss coefficient was converted into a stage efficiency loss using the following equations:

$$\eta' = \frac{\left(\frac{P'_5}{P'_{6.3}}\right)^{\frac{\gamma-1}{\gamma}} - \left[1 - \bar{e}_{S,T} + \bar{e}_{S,T}\left(\frac{P'_5}{P_{5.5}}\right)^{\frac{\gamma-1}{\gamma}}\right]\left[1 - \bar{e}_{R,1} + \bar{e}_{R,T}\left(\frac{P''_{5.5}}{P_{6.3}}\right)^{\frac{\gamma-1}{\gamma}}\right]}{\left(\frac{P'_5}{P'_{6.3}}\right)^{\frac{\gamma-1}{\gamma}} - 1}$$

For the stator:

$$\Delta\eta'_{stage} = 1 - \eta', \text{ when } \bar{e}_{R,T} = 0$$

For the rotor:

$$\Delta\eta'_{stage} = 1 - \eta' - \Delta\eta'_{stage}\ (\text{stator}), \text{ where } \bar{e}_{S,T,} \text{ and } \bar{e}_{R,T,} \neq 0$$

The stage efficiency losses for the stator and rotor were added to those for the manifold and exhaust duct to calculate an overall efficiency.

Since the boundary layer calculation used in the analysis implicitly applies to smooth surfaces only, the calculated profile and endwall friction losses were assumed those for smooth rotor blades. For this reason comparisons of the analytically calculated turbine flow characteristics were made only with the experimental results obtained for the turbines with smooth rotor blades.

RESULTS AND DISCUSSION

The performance of the redesigned turbine is presented in five parts. The results of the stator inlet survey are presented first followed by the overall stage performance for the as-cast blading. The effect of Reynolds number on the turbine performance is then presented followed by the change in efficiency for the polished rotor blades. Finally, the performance of this

turbine is compared, both analytically and experimentally, with the first turbine design.

Stator Inlet Surveys

Radial surveys of flow angle and total pressure were made at the stator inlet (station 5) at two circumferential locations (fig. 9) for manifold-inlet-total to stator-exit-static pressure ratios of nominally 1.38, 1.56, and 1.70. The results were similar for all three pressure ratios. The survey results obtained at a pressure ratio of 1.70 are shown in figure 10. The angle measurements are plotted in figure 10(a). The dashed line is the design radial variation in flow angle and the three filled-in symbols are the stator-inlet blade angles. The flow angle measured was generally between 40 and 50 degrees over most of the passage height but decreased near the endwalls. The largest deviation between design and measured flow angle occurred in the outer half of the passage height. Although the flow direction deviated appreciably from the design prediction, the net result was a significant reduction in stator incidence which benefited the stage performance. The shape of the radial variation in flow angle at location A suggests a CCW vortex being shed from the shroud lip (fig. 1). It is not known how far around the periphery flow was being shed from the shroud lip in this manner since much of the area CCW to location A was not accessable for surveying.

The radial variations in manifold-exit total pressure at the two survey locations are plotted in figure 10(b). The total pressure variations are slightly different between the two locations. There appears to be a slight decrease in pressure as the flow moves around the volute. Wall boundary layers were about 12 percent thick at the hub and 5 percent thick at the tip. By comparison the boundary layers for the first volute were about 20 percent thick at the hub and 15 percent thick at the tip. The shedding of the flow from the shroud lip at location A resulted in a local pressure loss from about 60 percent passage height to the shroud. The calculated mass average pressure loss in the manifold was 1/3 percent.

The radial variations in calculated mass flow at the two survey locations are shown in figure 11. The mass flows were calculated from the survey results and are expressed in terms of the mass flow parameter, ψ. The mass flow parameter is defined as:

$$\psi = \frac{(\Delta m)_{local}}{(\Delta m)_{av}} - 1$$

and was used to provide nondimensionalized numbers because of the difference between the design and measured mass flows. The $(\Delta m)_{local}$ was the calculated mass flow through each of 40 equal incremental flow areas. The $(\Delta m)_{av}$ was the summation of the calculated local mass flows divided by 40. The calculations were made assuming a linear variation in static pressure from hub to tip. The mass flow parameter, ψ, indicates the percentage deviation in the local mass flow from the average mass flow at a given radial and circumferential location. The dashed curve in the figure indicates the radial distribution in mass flow calculated from the design diagrams.

The total mass flow calculated for each of the two survey locations was within 3 percent of each other but differed markedly from design. The measured mass flow distribution compared to design had substantially less flow per unit area between the hub and about 60 percent span and substantially more flow per unit area from there to the tip. The change in the radial distribution of mass flow from that designed to the measured distribution was probably not detrimental to the turbine performance. The measured distribution indicated a shifting of mass flow away from the hub where losses were high. The general trend of more mass flow per unit area near the walls and less mass flow per unit area from about 10 percent to 60 percent span is similar to that found in the first volute design (ref. 3). Perhaps the ideal mass flow distribution would be to reduce the mass flow near the walls where the losses are the highest and increase it in midspan where the losses are low. This idealized mass distribution was not achieved in either volute design.

Performance of As-Cast Blading

Mass flow. - The variation in equivalent mass flow rate with equivalent total pressure ratio and speed is shown in figure 12. The equivalent design mass flow given in the figure is the design mass flow value for cold hardware that is listed in table I. The data show that the rotor choked before the stator for all speeds above 70 percent and thus controlled the turbine mass flow. The measured mass flow at design speed and the equivalent design pressure ratio of 2.048 was 0.311 kg/sec which is 1.2 percent less than the design flow. The rotor throat area was measured and found to be 1 percent too large. Therefore, the mass flow per unit area was 2.2 percent less than design.

Torque and specific work. - The variation in equivalent torque with equivalent pressure ratio and speed is presented in figure 13. At the equivalent design speed and pressure ratio, the measured equivalent torque was 4.91 N-m. This is 0.8 percent less than design. Since the mass flow was 1.2 percent less than design, the turbine specific work was 0.4 percent greater than design. This is illustrated in figure 14 which shows that at the equivalent design total pressure ratio of 2.048 and design rotor speed the work output of the turbine was 45,800 J/kg.

Efficiency. - The turbine efficiency is shown in figure 15. The two symbols on the figure indicate the design (filled-in) and a part power (open) condition. The estimated part power turbine operating parameters of speed and pressure ratio were calculated from data given in reference 4. The predicted part power efficiency was 0.84. At this part power condition the measured efficiency was 0.837 which is in very good agreement with the predicted value. At equivalent design speed and pressure ratio, the turbine efficiency was 0.854 which is slightly higher than the design goal of 0.85. Although the test efficiencies compare well with the goals, it should be noted that the experimental efficiencies were obtained with a tip clearance of 1.2 percent rather than the design tip clearance of 2 percent. The effect on efficiency of this tip clearance change is discussed in the section entitled Effect of rotor tip clearance.

Rotor-exit survey. - The results of the radial surveys at station 6.3 of flow angle, total pressure, and total temperature are shown in figures 16(a)

to (c). The measurements were taken with the turbine operating at equivalent design speed and specific work. The data shown are the measurements of the three survey probes. With these measurements, the radial variation in stage efficiency was calculated and is shown in figure 17. The dashed curves in the figures represent the calculated design radial variations at the turbine exit taken from the design report.

The measured flow angle (fig. 16(a)), shows the flow was turned more tangentially near the hub and shroud and less in midspan. Differences in magnitude and trends existed between the measured flow angle and the calculated design angle. Similar differences between design calculations and measurements are also evident for the pressure and temperature shown in figures 16(b) and (c). It appears that the blade shapes generated during the design were inadequate to establish the design flow conditions. However, a recent analytical recalculation of the turbine flow conditions for the blade shapes tested gave results that agreed much better with the measurements. That analysis is discussed later in this report.

The measured overall pressure ratio (fig. 16(b)), indicated a larger gradient from hub to midspan to tip than the design. The lowest pressure ratio occurred at midspan and the highest pressure ratios occurred at the hub and tip. The temperature measurements (fig. 16(c)), indicated very uniform work extraction radially and differed from the design intent.

The radial variation in efficiency (fig. 17), agrees very well with design. This result of achieving design efficiency while not establishing design flow gradients may be unexpected. However, the deviation in flow angle from design at the stator inlet reduced the inlet incidence. Also, the more uniform radial mass flow distribution (fig. 11), was probably beneficial. Finally, the design values of efficiency in figure 17 were calculated for a 2 percent rotor tip clearance whereas the test was made with a 1.2 percent tip clearance.

Effect of Reynolds Number

A Reynolds number test was made with the as-cast blading. As stated earlier the Reynolds number was varied by varying the turbine inlet pressure while holding the speed and pressure ratio constant. For each inlet pressure the Reynolds number and turbine efficiency were calculated, from smooth-curve data, at the design work factor of 2.1. The test results are shown in figure 18. The Reynolds number at the hot-engine design condition was 2.36×10^5. As the data indicate, no effect of Reynolds number was measured over the range covered.

Effect of Blade Surface Roughness

During the performance evaluation of the first turbine design (ref. 6), it was found that smoothing the as-cast rotor blade surface finish resulted in a one point gain in efficiency. The results of retesting the second turbine after smoothing the rotor blades are shown in figure 19. Overall performance was measured over a range of pressure ratios at equivalent design speed. Over the entire range of pressure ratios, the insertion of the polished rotor

resulted in nominally 1/2 point improvement in efficiency. This is one-half the improvement in efficiency measured with the first turbine design. Radial flow surveys taken at the exit of the polished rotor (station 6.3) showed results almost identical to those for the as-cast rotor.

Analytical Results

The objective of the loss analysis was to determine the reasons the second turbine performed better than the first turbine. This was done by calculating the individual loss components for the two turbines at the two operating conditions. Since the loss analysis procedure was largely theoretical, confidence in the final calculated losses is increased by experimentally verifying the calculations where possible. This was done by comparing the stage exit flow conditions and overall efficiencies calculated from the loss analysis with the exit flow conditions and efficiencies obtained from experimental data. Also, to assist in explaining the reason a calculated loss increased from one turbine to the other, blade surface velocity distributions are presented for both turbines for both operating conditions. The results are first presented for the design speed and work condition and then for the part power condition. The section ends with a discussion of the effect on turbine efficiency due to the difference in rotor tip clearance that existed between the two turbines.

Analysis at design speed and work. - The calculated velocity diagrams for the second turbine at the design work and speed condition are shown in figure 20. The design velocity diagrams from figure 3 are superimposed for comparison. A comparison of the calculated velocity diagrams with the design diagrams shows significant deviations. The calculated diagrams show larger velocities and flow angles at the stator exit (station 5.5) for all three radial sections. At the rotor exit (station 6.3) the results show lower relative velocities at the hub and mean sections and lower absolute velocities at all three sections.

A comparison of the analytically calculated rotor exit flow angles and velocities with those obtained from the rotor exit radial survey measurements is shown in figure 21. The experimental radial variations in velocities and flow angles were computed from the rotor exit survey for the smoothed blade. The dashed curves are the analytically calculated values. The agreement between the experimental and analytical results over most of the blade height is excellent. Some deviations exist at the hub and tip sections but the agreement is still considered good. Since MERIDL is an inviscid program that calculates flow properties along a hub to shroud midchannel stream surface, the best agreement would be expected away from the endwalls were viscous and tip clearance effects are not a factor. Since stator exit radial surveys were not made, a similar comparison between the analytical and experimental results at that location could not be made.

The surface velocities calculated in the loss analysis for the first and second stator designs are shown in figures 22(a) and 23(a), respectively. The design surface velocities are superimposed for comparison. For the first stator (fig. 22(a)), there were large velocity peaks near the leading edge on the suction surfaces of all three vane sections, followed by relatively constant velocities to the trailing edge. These velocity distributions differed

from the design distributions, because (1) the current results were obtained with a quasi-three-dimensional computation instead of the two-dimensional computation used in the design, (2) the stator geometry was changed to reflect the actual hardware, and (3) the stator inlet flow conditions were obtained from test measurements rather than design estimates.

The vane surface velocities calculated in the loss analysis for the redesigned stator, figure 23(a) showed moderate acceleration on the suction surface of the hub and mean sections. However, at the contoured tip section, the vane was unloaded over the first 25 percent of the chord. This was followed by a rapid acceleration to the 75 percent chord location and then large diffusion to the trailing edge. The crossing of the surface velocity curves near the trailing edge indicates excessive vane camber for the exit velocity diagram. Differences that exist between the surface velocities from the loss analysis and the design distributions are attributed to differences in the streamsheet thicknesses used for the two calculations. The calculations made for the analysis used the streamsheet thickness obtained from the MERIDL program which was not used when this stator was designed.

Figures 22(b) and 23(b) show the surface velocities calculated for the loss analysis for the first and second rotor designs, respectively, with the design variations superimposed for comparison. The first turbine rotor shows moderate diffusion on the suction and pressure surfaces of all three sections and good agreement with the design loading. The second rotor shows minimal diffusion at all three sections. Compared to the design variations, there was good agreement at the hub section, but only fair agreement at the mean and tip sections.

The results of the analytically calculated losses for the two turbines are shown in table VI. The stator losses include profile friction (including mixing), endwall friction, secondary flow, and incidence. The losses are tabulated in the same manner in the rotor with the inclusion of tip clearance loss. Two main conclusions can be drawn from this table. First, there was good agreement between the analytically calculated and experimental efficiencies for both turbines. Second, the analysis shows that most of the efficiency difference between the two turbines was due to reduced rotor losses for the second turbine. A discussion of the individual losses in the stator and rotor for the two turbines follows.

The total kinetic energy loss for the second stator, table VI, was only 0.003 less than that calculated for the first stator. In fact, the profile friction loss for the second stator was larger by 0.007 compared to the first stator, indicating that a benefit due to use of a contoured stator was apparently not realized. The reason for this is attributed to the surface velocity discussed in figures 22(a) and 23(a). For the first stator, the leading edge velocity peaks, although undesirable, did not substantially increase the calculated profile friction loss. For the second stator the hub and mean section profile losses were about the same as the first stator. However, there was a much higher profile loss calculated for the tip section due to the unfavorable velocity distribution. The other three stator losses were lower for the second stator, particularly the incidence loss. Due to the lower stator pressure ratio of the second turbine compared to the first turbine the small reduction in the stator total kinetic energy loss for the redesigned turbine resulted in a 0.008 increase in stage efficiency.

Table VI shows that for the second rotor design there was a 0.050 lower total kinetic energy loss coefficient. This 0.050 difference translated into a 0.034 increase in stage efficiency. All five loss categories for this rotor were lower than the first rotor. The lower profile and endwall friction losses are consistent with the lower diffusion of the second rotor compared to the first rotor shown in figures 22(b) and 23(b).

Analysis at part power. - The stator and rotor surface velocities are shown in figure 24 for the first turbine at the part power condition. The surface velocities calculated in the loss analysis at the design speed and work condition (fig. 22), are included for reference. The stator suction surface velocities did not show peaks near the leading edge as large as those at the design speed and work condition. Also, the stator exit velocity ratios were less, resulting in slightly more diffusion. The rotor blade surface velocities showed larger differences between the two flow conditions. The lower level of rotor reaction at the off-design condition caused larger friction losses.

The stator and rotor surface velocities for the second turbine at the part power condition are shown in figure 25. The stator surface velocities showed slight differences between the two flow conditions. The rotor surface velocities showed much larger differences with the suction surface velocities for the part power condition showing much less acceleration. This, in turn, caused higher profile and endwall friction losses.

The tabulated results of the loss analyses for the two turbines operating at the part power condition are given in table VII. For this operating condition, the experimental stage efficiencies for both turbines were obtained from performance data for the as-cast versions of both turbines with adjustments made to account for efficiency improvements due to reworking and/or polishing the rotor blades. The calculated stage efficiency for the second turbine agrees well with the experimental value. However, for the first turbine the calculated efficiency was nearly two points lower than the experimental value.

A comparison of the losses for the first turbine at the two operating conditions, tables VI and VII, showed increased stator losses at the part power condition due mostly to increased surface friction and incidence losses. The increased stator losses caused a reduction in stage efficiency of about two points. All of the rotor losses except for the rotor tip clearance loss were also significantly higher at the part power condition. The primary cause for the increased losses was the rotor incidence loss. The rotor inlet relative flow angles for the part power condition ranged from 4° to 9° larger than at the design speed and work condition.

Similar conclusions can be drawn for the second turbine in comparing the losses for the two operating conditions. The stator loss increased slightly for the part power condition, which resulted in about a one point decrease in stage efficiency. The rotor total loss increased by about 0.04, also causing about a one point decrease in stage efficiency. As with the first turbine, the primary cause for the increased rotor losses was due to rotor incidence.

Effect of rotor tip clearance. - The larger tip clearance losses for the first rotor listed in tables VI and VII were due to a larger tip clearance

(1.7 percent of the rotor blade height compared to 1.2 percent for the second rotor). Two additional cases were analyzed to predict the increase in tip clearance loss for the redesigned turbine for rotor tip clearances equal to 1.7 and 2.0 percent of the rotor blade height. The calculations were made for the design speed and work condition. The 1.7 percent case was done to match the rotor tip clearance for the first turbine. The 2.0 percent case was done to match the design clearance value. For the 1.7 percent case, the kinetic energy loss due to tip clearance increased to 0.056 resulting in an additional reduction in overall stage efficiency of 0.011. For the 2.0 percent case, the kinetic energy loss increased to 0.066 resulting in an additional reduction in overall stage efficiency of 0.018.

Based on the results discussed above, if the 0.011 reduction in stage efficiency were applied to the experimental results, a measured stage efficiency of 0.848 would be predicted for the second turbine at a tip clearance of 1.7 percent. This projected efficiency would be 2.3 points higher than the initial turbine efficiency at the same clearance. Similarly, at the design level of rotor tip clearance (2.0 percent) a measured stage efficiency of 0.841 would be predicted, which is slightly less than the design goal of 0.85.

CONCLUDING REMARKS

The results of the compressor-drive turbine test series showed that good efficiency can be obtained with a small highly-loaded axial turbine. A potential improvement in efficiency, above that so far measured, exists as improved computer codes are developed and with better control in blading fabrication. For example, neither inlet manifold design generated flow conditions at the stator inlet that the design analysis predicted. However, the deviations from design at the manifold exit (stator inlet) for the second turbine design likely benefited the turbine performance. Also, the series of tests made with only small hardware changes (i.e., smoothing the blade surfaces and, in the case of the first design, reworking the blade profiles) illustrates the criticality of having very accurately made airfoils in small machines.

Analysis of the test results of the two turbines indicated that most of the improvement in performance of the redesigned turbine occurred in the rotor. The calculated stator kinetic energy loss for the two turbines was virtually the same. Rotor kinetic energy losses due to profile and endwall friction, mixing, and secondary flow were lower in the redesigned turbine. It appears then that the higher efficiency of the second design, at the same tip clearance, was primarily due to higher rotor reaction and reduced rotor blade diffusion. Benefits due to the contoured stator wall, larger volume inlet manifold and the parabolic work distribution were not apparent.

SUMMARY OF RESULTS

The aerodynamic performance of a redesigned compressor-drive turbine of the Department of Energy Upgraded Gas Turbine engine was determined in air at a nominal inlet temperature of 325 K. Two versions of the rotor were tested: an as-cast rotor and the same rotor with reduced surface roughness. Reynolds number tests were made for the as-cast rotor by varying the inlet pressure from 0.4 to 1.6 bars absolute. The results of the investigation were as follows:

1. The turbine efficiency values at design speed and work were 0.854 and 0.859 for the as-cast and reduced roughness rotors, respectively. An analysis of the smooth rotor at a tip clearance of 1.7 percent indicated an efficiency of 0.848. This compares to an efficiency of 0.825 for the initially designed turbine at the same tip clearance. At the design tip clearance of 2.0 percent a turbine efficiency of 0.841 was indicated for the reduced roughness rotor configuration. There was no change in efficiency with Reynolds number.

2. An analysis of the two turbines indicated that the primary cause of the performance improvement of the redesigned turbine was lower surface friction, mixing, and secondary flow losses in the rotor.

3. The measured efficiency at part power decreased only moderately and agreed well with the part power prediction.

4. The effect of several features incorporated in the redesigned turbine to reduce the aerodynamic losses were inconclusive. These include a larger volume inlet volute, a contoured stator shroud, and parabolic work distribution.

REFERENCES

1. Ball, G. A.; Gumaer, J. I.; and Sebestyen, T. M.: The ERDA/Chrysler Upgraded Gas Turbine Engine Objectives and Design. SAE Paper 760279, Aug. 1976.
2. Roelke, R. J.; and McLallin, K. L.: The Aerodynamic Design of a Compressor-Drive Turbine for Use in a 75 kW Automotive Engine. NASA TM X-71717, 1975.
3. Roelke, R. J.; and Haas, J. E.: Cold-Air Performance of Compressor-Drive Turbine of Department of Energy Upgraded Automobile Gas Turbine Engine. I--Volute-Manifold and Stator Performance. NASA TM-82682, 1981.
4. Wagner, C. E.; and Pampreen, R. C.: Upgraded Automotive Gas Turbine Engine Design and Development Program, Vol. 2: Final Report. (COO-2749-43-VOL-2, Chrysler Corp.; EY-76-C-02-2749.) NASA CR-159671, 1979.
5. Horvath, D.; et al: Test Results of the Chrysler Upgraded Automative Gas Turbine Engine - Initial Design. NASA TM-81660, 1981.
6. Roelke, R. J.; and Haas, J. E.: Cold-Air Performance of Compressor-Drive Turbine of Department of Energy Upgraded Automobile Gas Turbine Engine. II--Stage Performance. NASA TM-82818, 1982.
7. Roelke, R. J.; and Haas, J. E.: The Effect of Rotor Blade Thickness and Surface Finish on the Performance of a Small Axial Flow Turbine. ASME Paper 82-GT-222, Apr. 1982.
8. Katsanis, T.: FORTRAN Program for Calculating Transonic Velocities on a Blade-to-Blade Stream Surface of a Turbomachine. NASA TN D-5427, 1969.
9. Boyle, R. J.; and Haas, J. E.; Katsanis, T.: Comparison Between Measured and Predicted Turbine Stage Performance and Predicted Performance Using Quasi-3D Flow and Boundary Layer Analyses. NASA TM-83640, 1984.
10. Katsanis, T.; and McNally, W. D.: Revised FORTRAN Program for Calculating Velocities and Streamlines on the Hub-Shroud Midchannel Stream Surface of an Axial-, Radial-, or Mixed-Flow Turbomachine or Annular Duct. I--User's Manual, NASA TN D-8430, 1977.

11. McNally, W. D.: FORTRAN Program for Calculating Compressible Laminar and Turbulent Boundary Layers in Arbitrary Pressure Gradients. NASA TN D-5681, 1970.

TABLE I. - TURBINE DESIGN PARAMETERS

Parameter	Equivalent			
	Hot engine	Hot hardware	Cold hardware	Component test
Turbine-inlet temperature, K	1325	288.2	288.2	325
Turbine-inlet pressure, bars	4.04	1.01	1.01	0.83
Mass flow rate, kg/sec	0.588	0.323	0.315	0.242
Rotative speed, rpm	58 500	27 673	27 673	29 386
Specific work, J/kg	203 700	45 600	45 600	51 400
Torque, N m	19.5	5.09	4.95	4.03
Power, kW	119.7	14.7	14.3	12.4
Total pressure ratio, $p'_{4.5}/p'_{6.3}$	1.982	2.048	2.048	2.048
Total efficiency, η'	0.85	0.85	0.85	0.85
Work factor, $\Delta h/U_m^2$	2.10	2.10	2.16	2.16
Reynolds number, $m/\mu r_m$	236 000	355 930	351 000	244 000
Mean blade speed, m/sec	311.7	147.4	145.4	154.4

TABLE II. - STATOR DESIGN PARAMETERS

Parameter	Hub	Mean	Tip
Profile radius at T.E., cm	4.445	5.107	5.730
Actual chord, cm	2.591	3.023	3.810
Axial chord, cm	1.449	1.269	1.506
Leading edge radius, cm	0.060	0.050	0.090
Trailing edge radius, cm	0.019	0.019	0.019
Trailing edge blockage, percent	5.0	5.9	5.8
Inlet blade angle, deg	29.2	45.0	38.7
Incidence, deg	-11.2	-4.1	-17.2
Exit blade angle, deg	64.3	71.6	73.2
Solidity, c/s	1.39	1.41	1.59
Blade number	-----	15	-----
Blade height at T.E., cm	-----	1.285	-----
Aspect ratio, AR	-----	0.43	-----

TABLE III. - ROTOR DESIGN PARAMETERS

Parameter	Hub	Mean	Tip
Profile radius, cm	4.445	5.088	5.730
Actual chord, cm	1.085	1.058	1.035
Axial chord, cm	1.022	1.002	.852
Leading edge radius, cm	0.028	0.028	0.020
Trailing edge radius, cm	0.020	0.019	0.015
Trailing edge blockage, percent	16.2	14.2	11.9
Inlet blade angle, deg	47.0	51.6	27.8
Incidence, deg	-6.8	-6.1	-7.2
Exit blade angle, deg	58.0	59.8	65.1
Solidity, c/s	2.33	1.98	1.725
Blade number	-----	60	-----
Blade height, cm	-----	1.285	-----
Aspect ratio, AR	-----	1.215	-----

TABLE IV. - COMPARISON OF COMPRESSOR-DRIVE TURBINE DESIGNS

Parameter	First design	Second design
STAGE:		
Mass flow rate, kg/sec	0.598	0.588
Specific work, J/kg	198 100	203 700
Work factor, $\Delta h/U_m^2$	2.1	2.1
Flow factor, Vx/Um	0.88	0.73
Exit swirl at mean, deg	21.0	30.9
Reynolds number, $m/\mu r_m$	2.44×10^5	2.44×10^5
MANIFOLD:		
Type	volute	volute
Inlet velocity ratio, $(V/V_{cr})_{4,5}$	0.150	0.080
Exit velocity ratio, $(V/V_{cr})_5$	0.405	0.277
STATOR:		
Shroud type	cylindrical	contoured
Average reaction, Rx	0.593	0.566
Average solidity, c/s	1.10	1.46
Aspect ratio, AR	0.484	0.430
Trailing edge thickness, cm	0.038	0.038
Average t. e. blockage, percent	4.4	5.6
ROTOR:		
Tip diameter, cm	11.1	11.46
Blade length, cm	1.13	1.28
Average reaction, Rx	0.246	0.373
Average solidity, c/s	1.86	2.01
Aspect ratio, AR	1.219	1.215
Tip clearance, percent	2.2	2.0
Trailing edge thickness, cm	0.38	0.036
Average t. e. blockage, percent	12.0	14.0

TABLE V. - ROTOR SURFACE FINISH COMPARISON

Blade Surface	First design		Second design	
	Suction	Pressure	Suction	Pressure
As-Cast Finish, m x 10^{-6}	1.4	1.4	2.0	2.0
Reduced roughness finish, m x 10^{-6}	0.3	1.0	0.2	0.9

TABLE VI. - COMPARISON OF ANALYTICALLY CALCULATED LOSSES AT DESIGN EQUIVALENT SPEED AND WORK

	First design	Second design
STATOR LOSSES ($\bar{e}_S$):		
Profile Friction	0.017	0.024
Endwall Friction	.021	.019
Secondary	.008	.006
Incidence	.010	.004
Total	.056	.053
$\Delta\eta'$stage	0.047	0.038
$P'_5/P_{5.5}$	1.86	1.69
ROTOR LOSSES ($\bar{e}_R$):		
Profile Friction	0.061	0.048
Hub Endwall Friction	.014	.008
Secondary	.039	.026
Incidence	.016	.005
Tip Clearance	.047	.040
Total	.177	.127
$\Delta\eta''$stage	0.116	0.082
$P''_{5.5}/P_{6.3}$	1.61	1.57
MANIFOLD LOSS, $\Delta\eta'$stage	0.004	0.004
EXHAUST DUCT LOSS, $\Delta\eta'$stage	0.005	0.006
CALCULATED OVERALL EFFICIENCY	0.828	0.870
MEASURED OVERALL EFFICIENCY	0.825	0.859

TABLE VII. - COMPARISON OF ANALYTICALLY CALCULATED LOSSES AT 70 PERCENT EQUIVALENT DESIGN SPEED AND A STAGE PRESSURE RATIO OF 1.45

	First design	Second design
STATOR LOSSES ($\bar{e}_S$):		
Profile Friction	0.019	0.023
Endwall Friction	.026	.021
Secondary	.009	.006
Incidence	.013	.005
Total	.067	.055
$\Delta\eta$'stage	.068	.050
$P_5'/P_{5.5}$	1.47	1.42
ROTOR LOSSES ($\bar{e}_R$):		
Profile Friction	0.071	0.059
Hub Endwall Friction	.021	.012
Secondary	.051	.027
Incidence	.044	.032
Tip Clearance	.047	.040
Total	.234	.169
$\Delta\eta$'stage	.128	.091
$P_{5.5}''/P_{6.3}$	1.23	1.22
MANIFOLD LOSS, $\Delta\eta$'stage	0.010	0.008
EXHAUST DUCT LOSS, $\Delta\eta$'stage	0.004	0.004
CALCULATED OVERALL EFFICIENCY	0.790	0.847
EXPERIMENTAL OVERALL EFFICIENCY	0.807	0.843

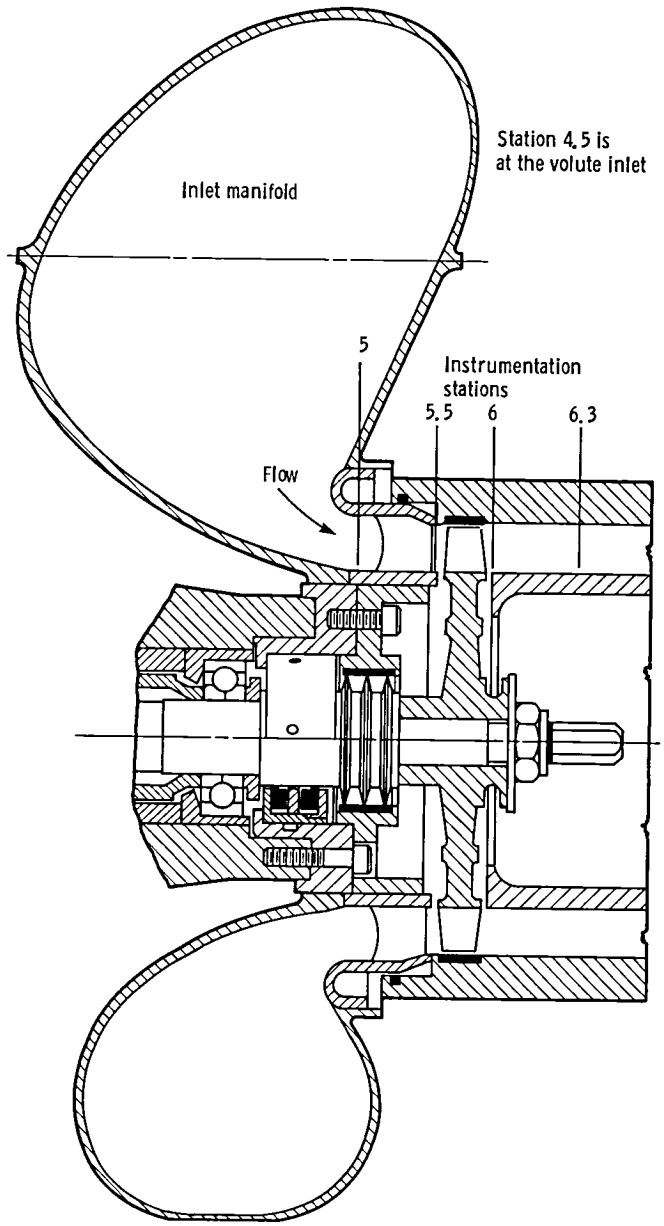

Figure 1. - Cross section of redesigned compressor-drive turbine.

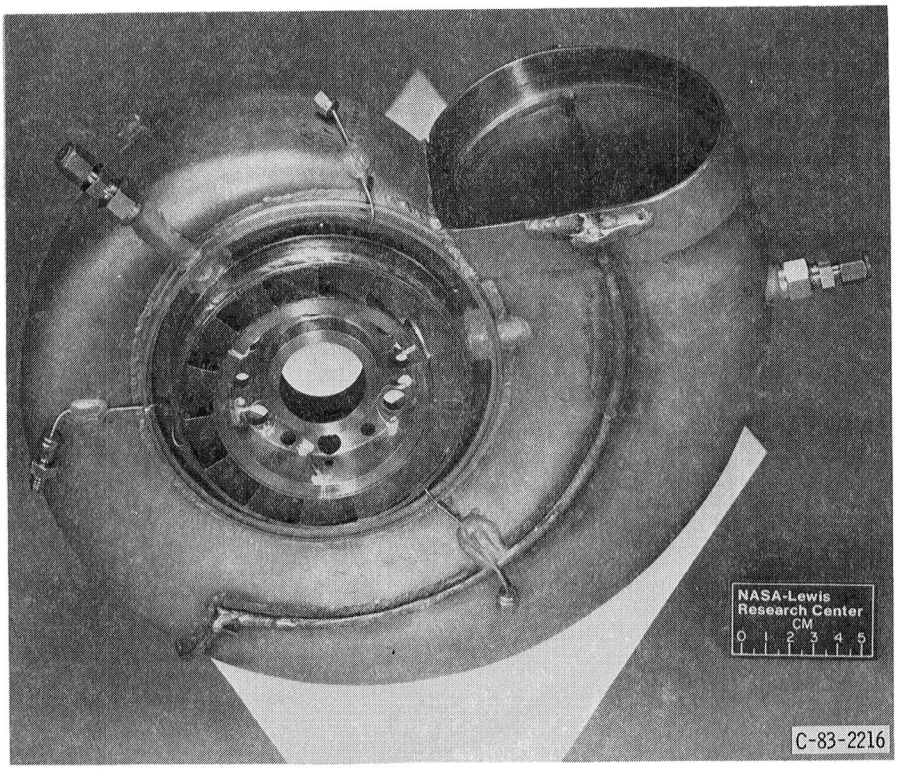

(a) Inlet volute and stator assembly.

Figure 2. - Test hardware.

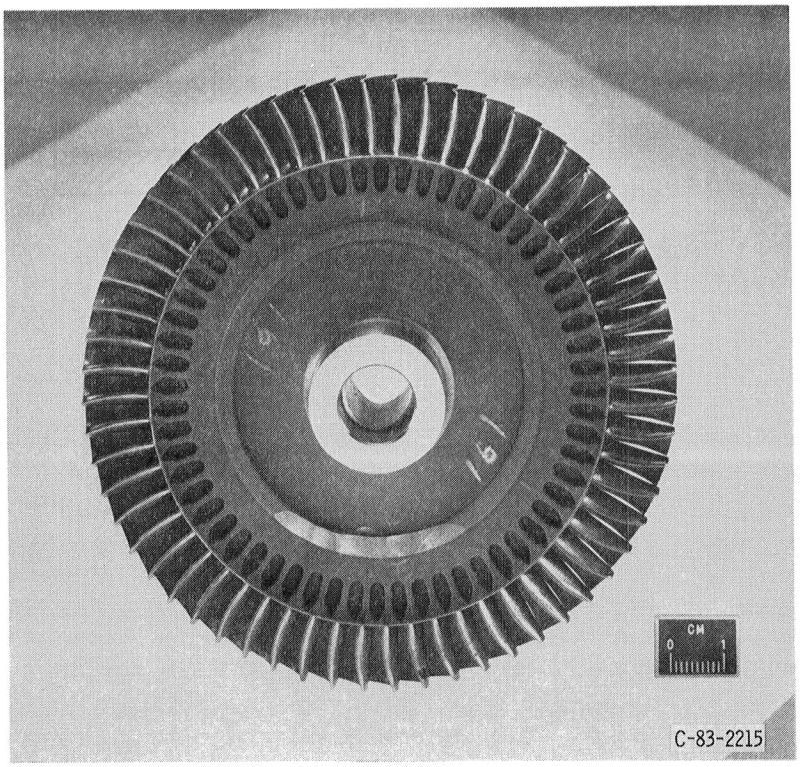

(b) Rotor.

Figure 2. - Concluded.

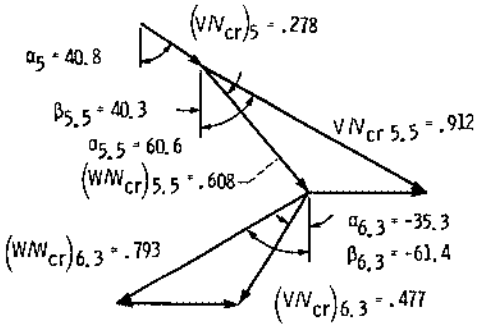

(a) 0% Streamline (hub).

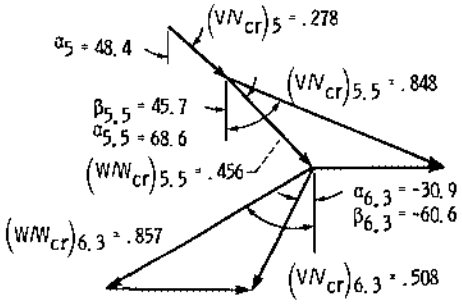

(b) 50% Streamline.

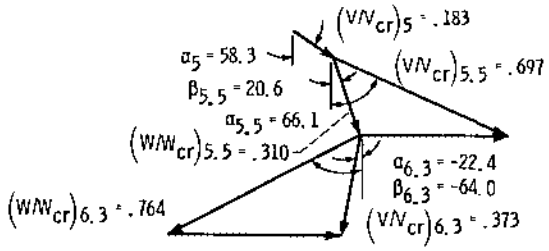

(c) 100% Streamline (tip).

Figure 3. - Design velocity diagrams.

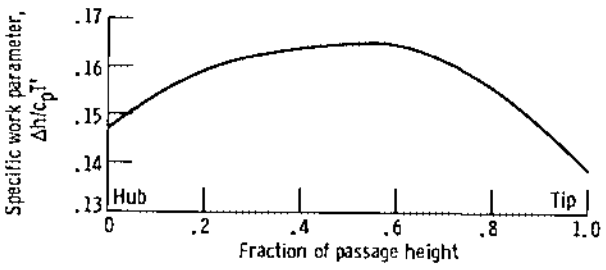

Figure 4. - Radial work distribution.

(a) Hub. (b) Mean. (c) Tip (r = 5.73 cm)

Figure 5. - Blading profiles and flow passages.

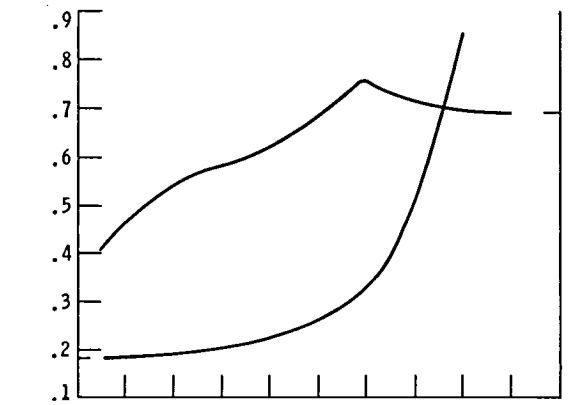

(a) Tip section.

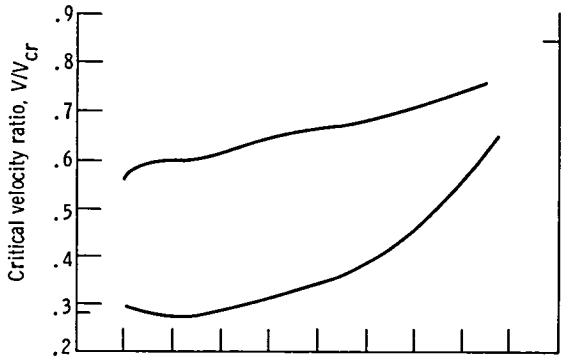

(b) Mean section.

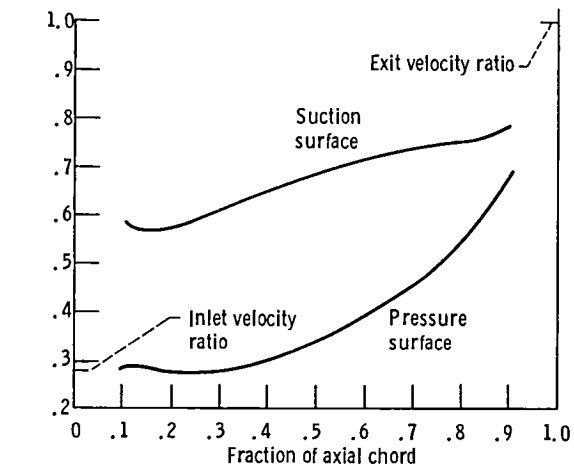

(c) Hub section.

Figure 6. - Stator vane design surface velocity distributions.

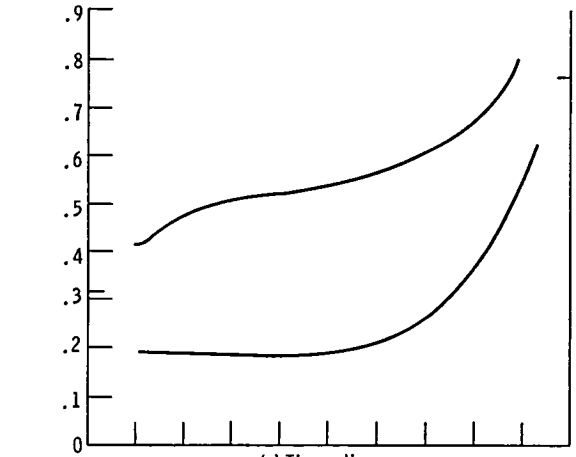

(a) Tip section.

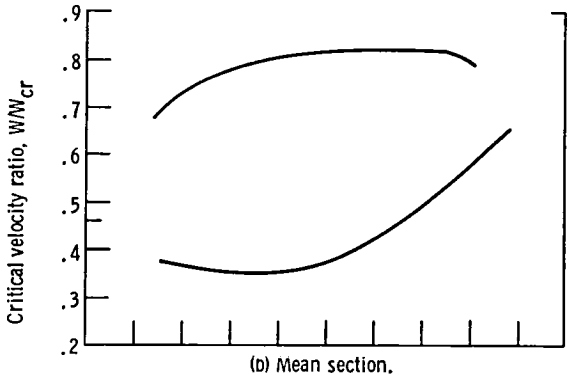

(b) Mean section.

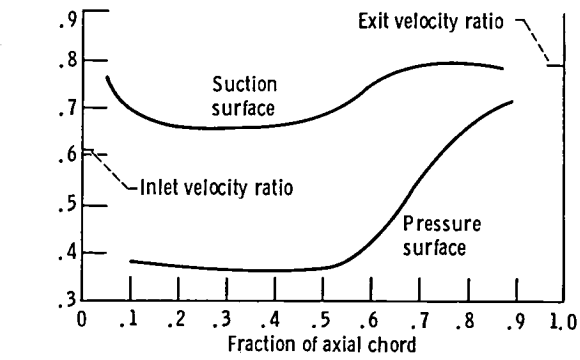

(c) Hub section.

Figure 7. - Rotor blade design surface velocity distributions.

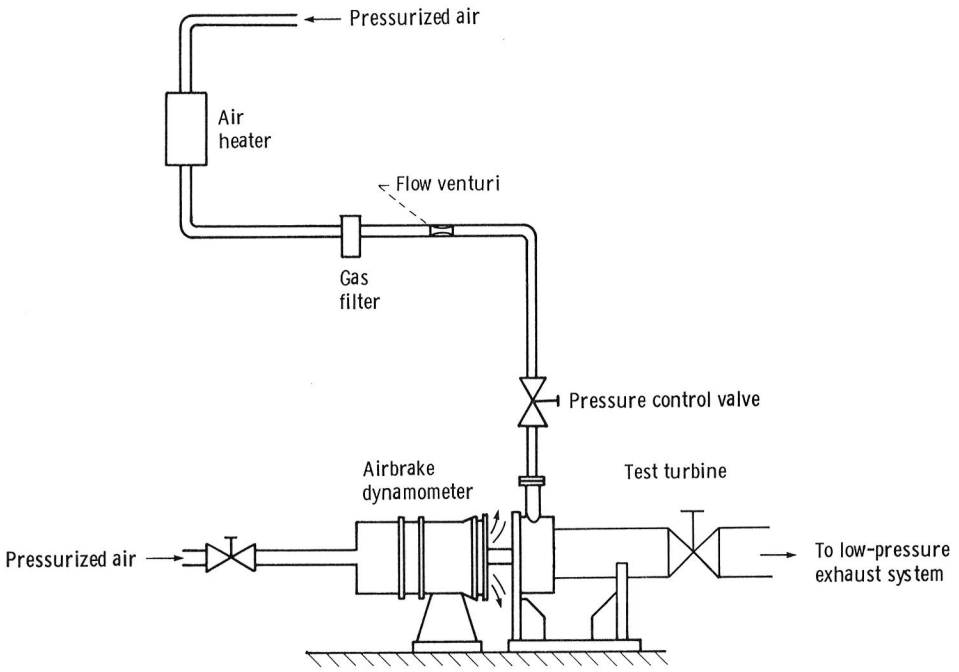

(a) Facility schematic.

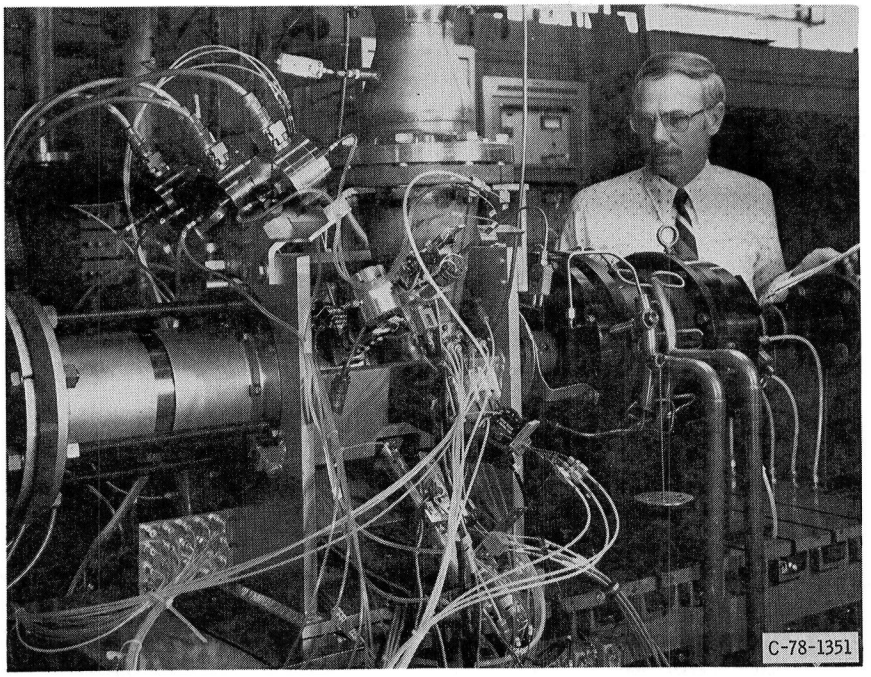

(b) Turbine test apparatus.

Figure 8.

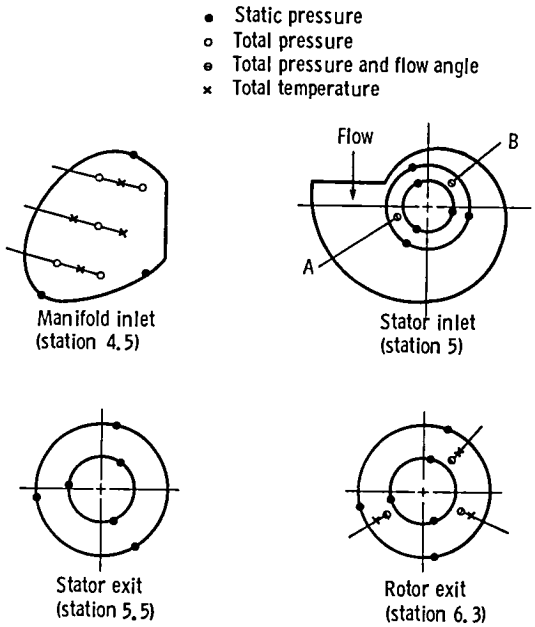

Figure 9. - Flow path instrumentation, viewed looking downstream.

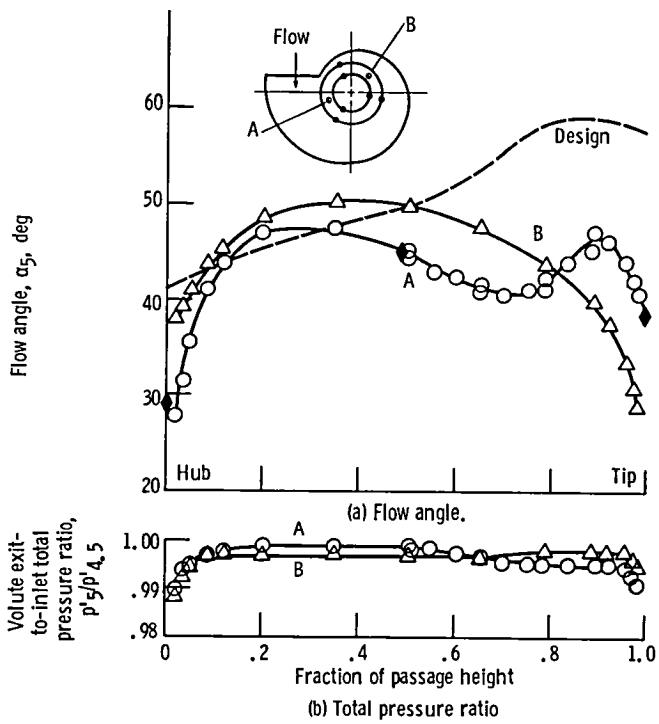

Figure 10. - Variation of volute exit flow angle and total pressure with radial position.

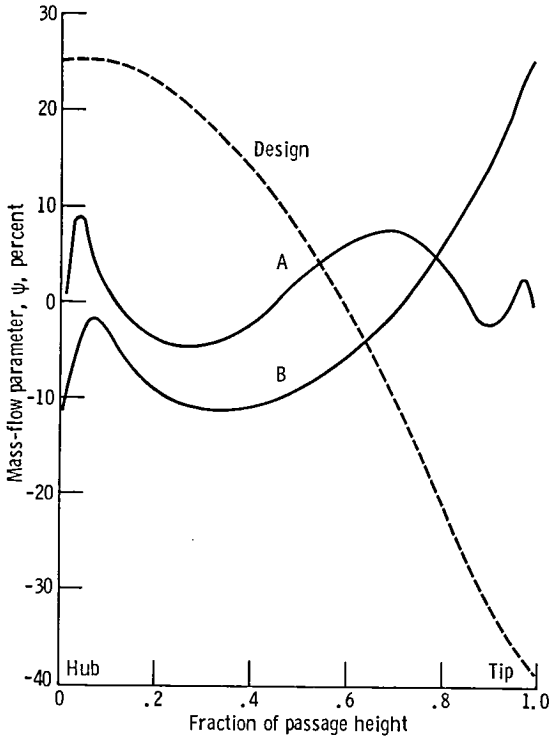

Figure 11. - Radial variation in mass flow parameter at the volute exit.

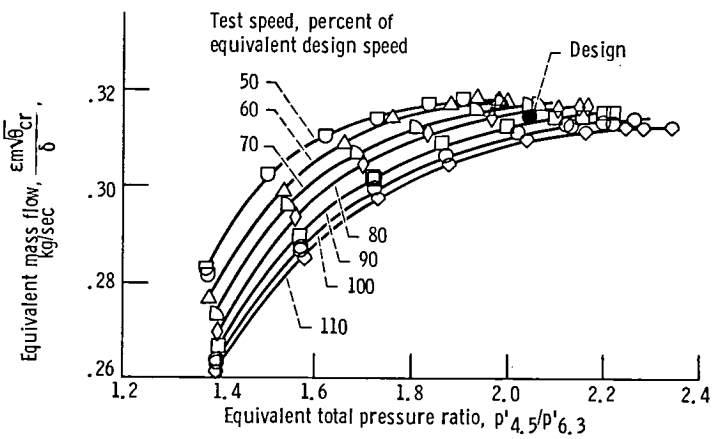

Figure 12. - Variation of equivalent mass flow with total pressure ratio and speed.

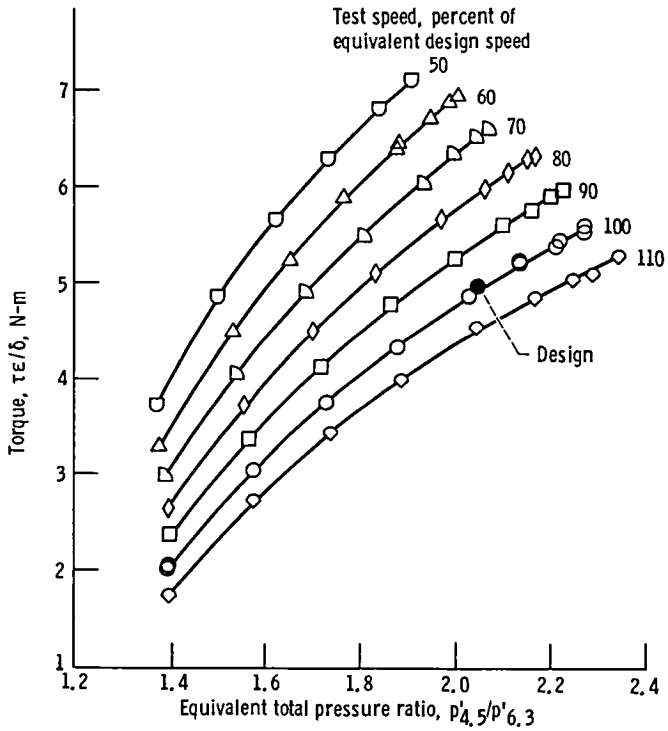

Figure 13. - Variation of torque with total pressure ratio and speed.

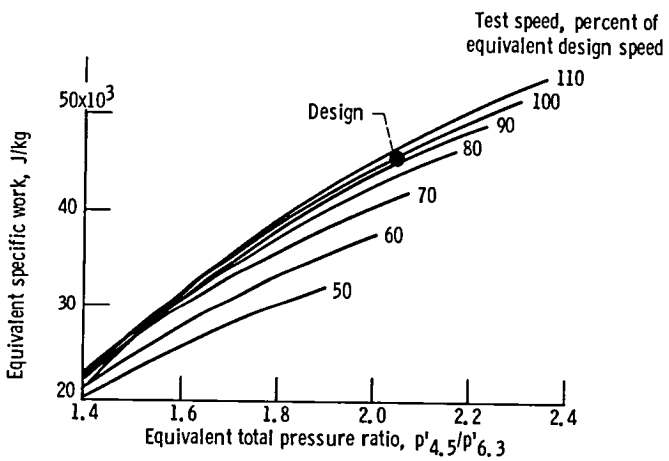

Figure 14. - Turbine specific work.

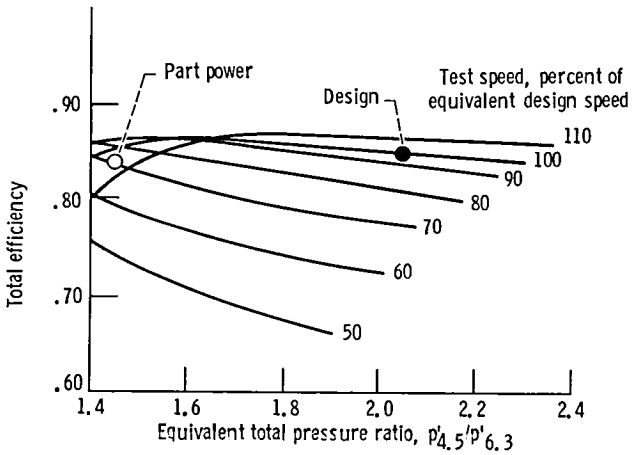

Figure 15. - Turbine total efficiency.

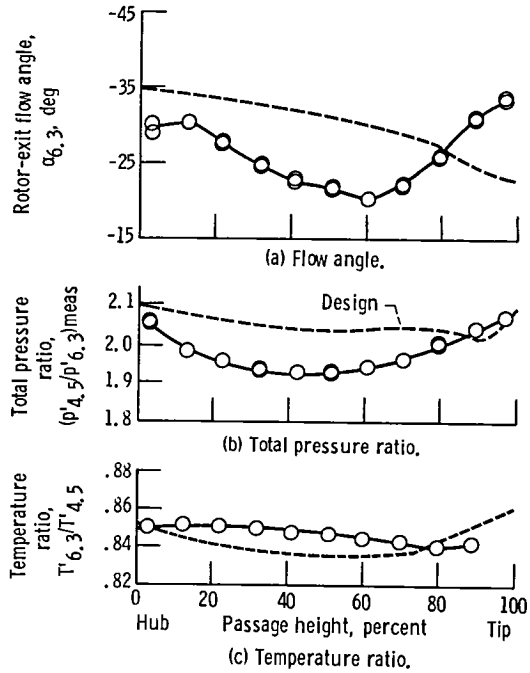

Figure 16. - Turbine exit survey.

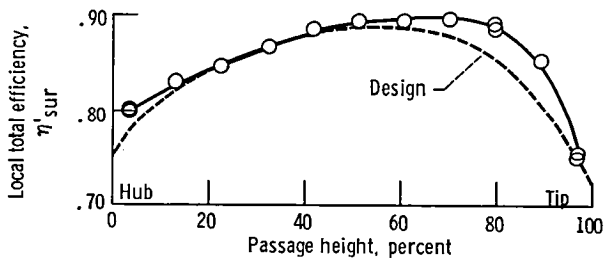

Figure 17. - Radial variation in total efficiency.

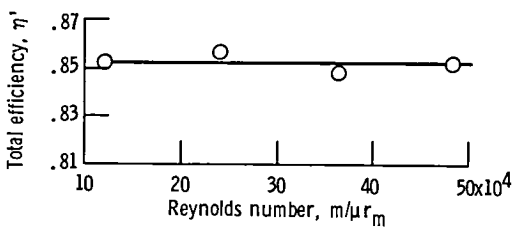

Figure 18. - Effect of Reynolds number on turbine efficiency.

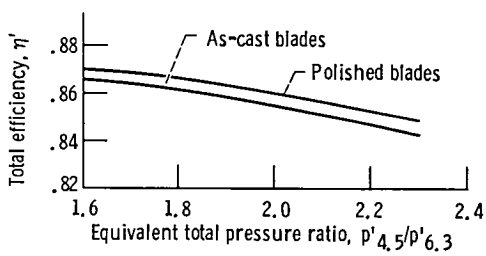

Figure 19. - Turbine total efficiency for as-cast and polished rotor blades.

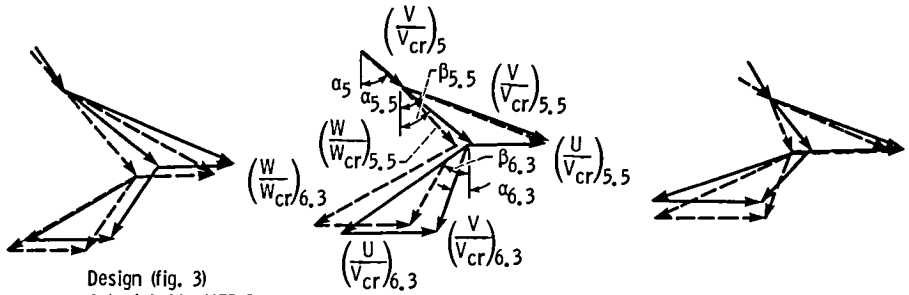

	Design (fig. 3)	Calculated by MERIDL for loss analysis	
$(V/V_{cr})_5$	.279	.252	.225
α_5	34.7	48.7	30.5
$(V/V_{cr})_{5.5}$	.973	.876	.786
$(W/W_{cr})_{5.5}$	.651	.490	.358
$(U/V_{cr})_{5.5}$	.410	.467	.529
$\alpha_{5.5}$	66.4	69.7	69.8
$\beta_{5.5}$	51.1	49.5	37.5
$(V/V_{cr})_{6.3}$	.459	.490	.357
$(W/W_{cr})_{6.3}$	.775	.786	.825
$(U/V_{cr})_{6.3}$	.445	.508	.580
$\alpha_{6.3}$	-34.9	-19.2	-43.1
$\beta_{6.3}$	-62.0	-55.4	-72.4
	Hub	Mean	Tip

Figure 20. - Comparison of design velocity diagrams with those calculated for loss analysis.

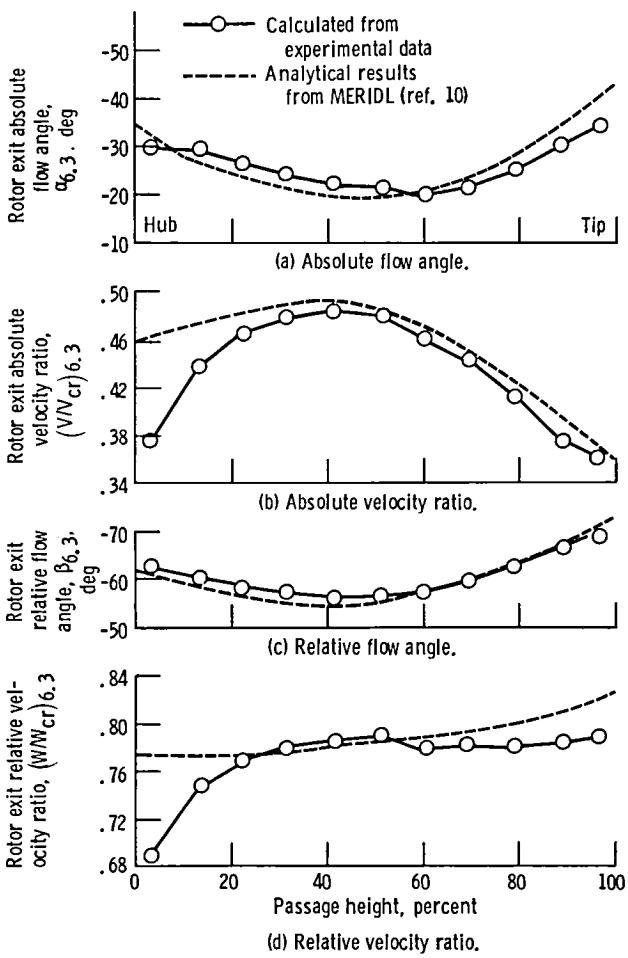

Figure 21. - Comparison of analytical and experimental rotor exit flow angles and velocity ratios.

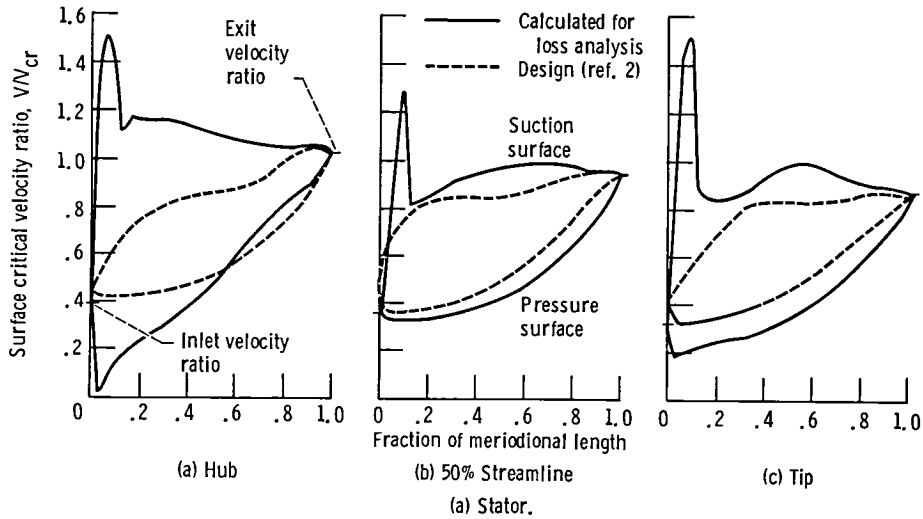

(a) Stator.

Figure 22. - Comparison of design and recalculated stator and rotor blade surface velocity distributions for the first turbine at equivalent design speed and work.

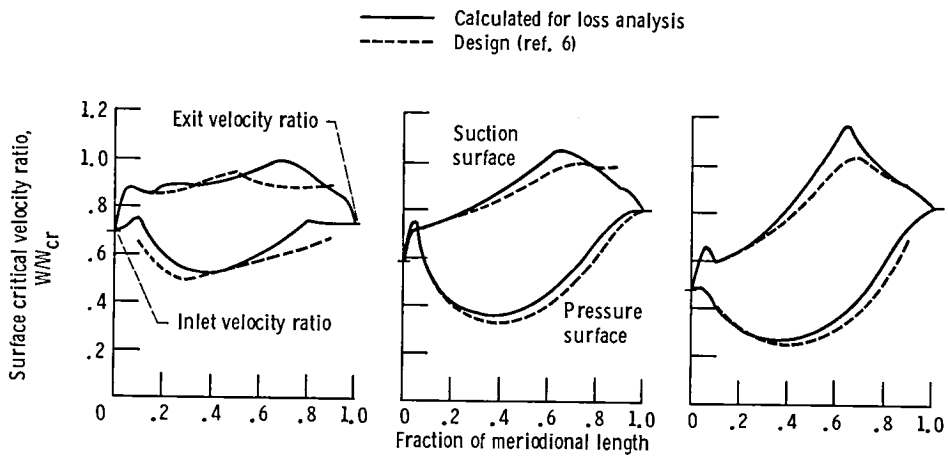

(b) Rotor.

Figure 22. - Concluded.

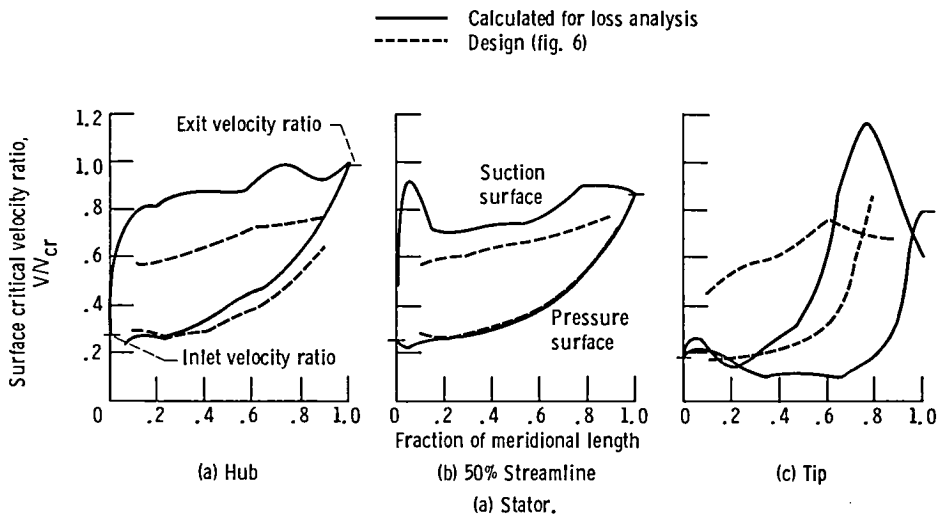

(a) Stator.

Figure 23. - Comparison of design and recalculated stator and rotor blade surface velocity distributions for the second turbine at equivalent design speed and work.

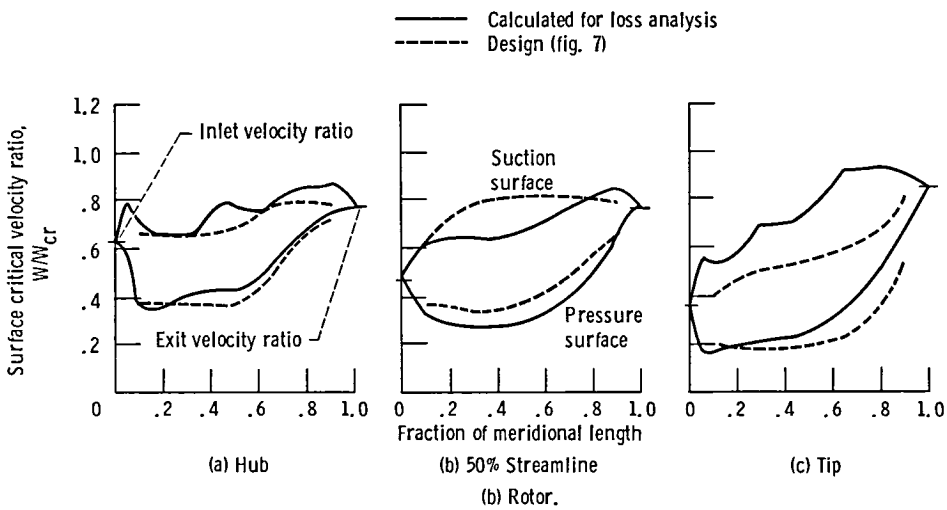

(b) Rotor.

Figure 23. - Concluded.

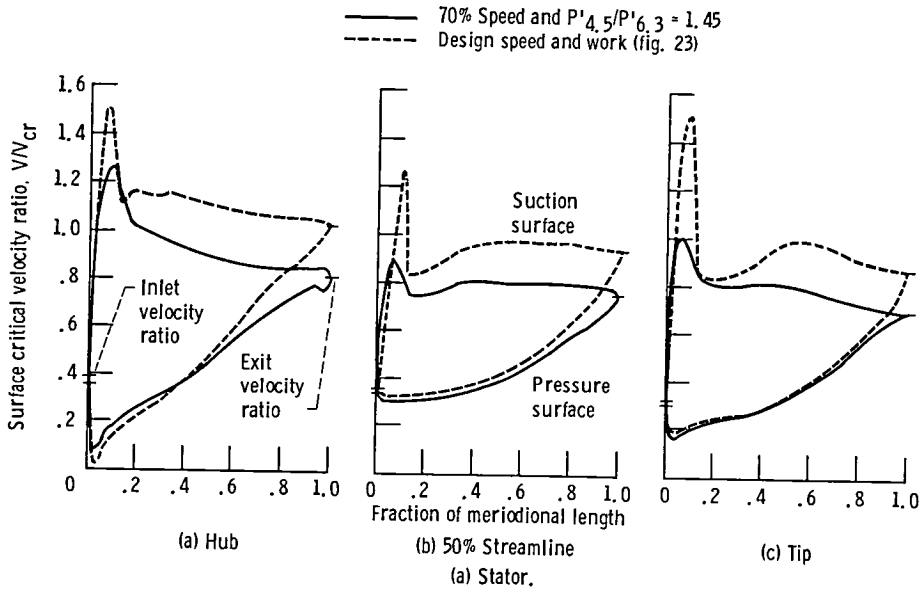

Figure 24. - Comparison of the design and recalculated stator and rotor surface velocity distributions for the first turbine at 70 percent equivalent design speed and a stage pressure ratio of 1.45.

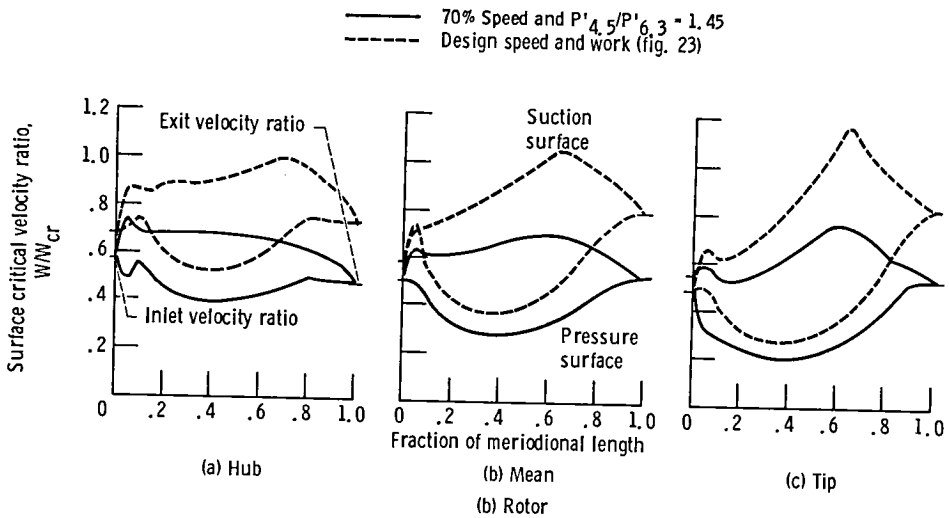

Figure 24. - Concluded.

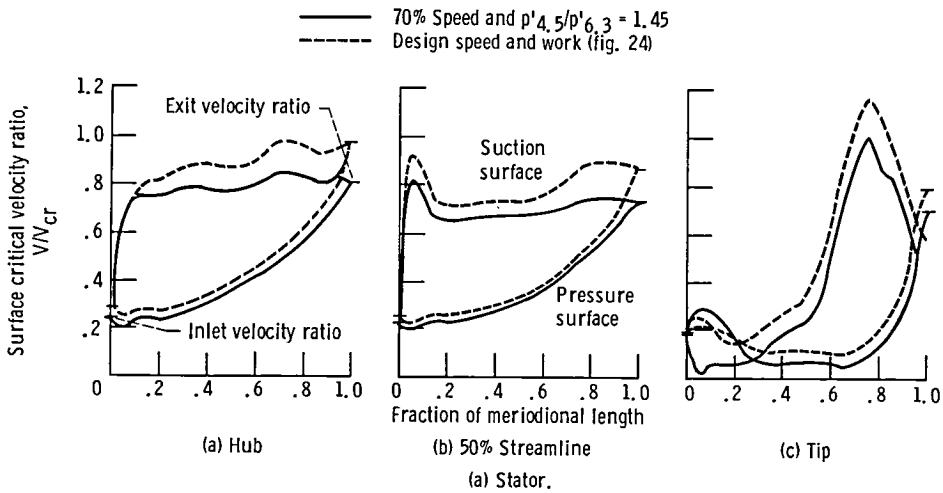

(a) Stator.

Figure 25. - Comparison of the design and recalculated stator and rotor surface velocity distributions for the second turbine at 70 percent equivalent design speed and a stage pressure ratio of 1.45.

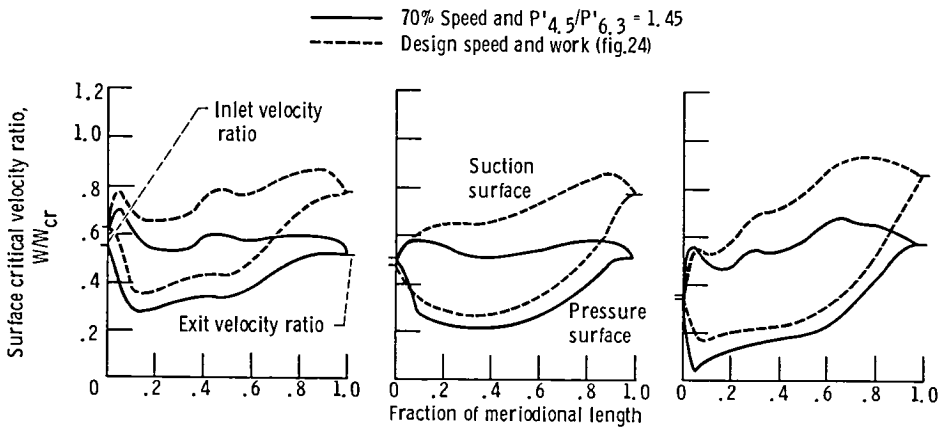

(b) Rotor.

Figure 25. - Concluded.

1. Report No. NASA TM-83627 USAAVSCOM TR-84-C-7	2. Government Accession No.	3. Recipient's Catalog No.

4. Title and Subtitle	5. Report Date
Cold-Air Performance of Compressor-Drive Turbine of Department of Energy Upgraded Automobile Gas Turbine Engine III - Performance of Redesigned Turbine	May 1984
	6. Performing Organization Code 778-32-01
7. Author(s) Richard J. Roelke and Jeffrey E. Haas	8. Performing Organization Report No. E-2044
	10. Work Unit No.
9. Performing Organization Name and Address NASA Lewis Research Center and U.S. Army Research and Technology Laboratories (AVSCOM) Cleveland, Ohio 44135	11. Contract or Grant No.
	13. Type of Report and Period Covered Technical Memorandum
12. Sponsoring Agency Name and Address U.S. Department of Energy Office of Vehicle and Engine R&D Washington, D.C. 20545	14. Sponsoring Agency ~~Code~~ Report No. DOE/NASA/50194-39

15. Supplementary Notes

Richard J. Roelke, NASA Lewis Research Center; Jeffrey E. Haas, Propulsion Laboratory, U.S. Army Research and Technology Laboratories (AVSCOM). Prepared under Interagency Agreement DE-AI01-80CS50194.

16. Abstract

The aerodynamic performance of a redesigned compressor-drive turbine of the Department of Energy Upgraded Gas Turbine engine was determined in air at nominal inlet conditions of 325 K and 0.8 bar absolute. The turbine was designed with a lower flow factor, higher rotor reaction and a redesigned inlet volute compared to the first turbine. Comparisons between this turbine and the originally designed turbine showed about 2.3 percentage points improvement in efficiency at the same rotor tip clearance. Two versions of the same rotor were tested: an as-cast rotor and the same rotor with reduced surface roughness. The effect of reducing surface roughness was about one-half percentage point improvement in efficiency. Tests made to determine the effect of Reynolds number on the turbine performance showed no effect for the range from 100 000 to 500 000.

17. Key Words (Suggested by Author(s))	18. Distribution Statement
Turbine engines Axial flow turbines Automobile engines	Unclassified - unlimited STAR Category 02 DOE Category UC-96

19. Security Classif. (of this report)	20. Security Classif. (of this page)	21. No. of pages	22. Price*
Unclassified	Unclassified		A02

*For sale by the National Technical Information Service, Springfield, Virginia 22161

National Aeronautics and
Space Administration

Washington, D.C.
20546

Official Business
Penalty for Private Use, $300

SPECIAL FOURTH CLASS MAIL
BOOK

Postage and Fees Paid
National Aeronautics and
Space Administration
NASA-451

NASA

POSTMASTER: If Undeliverable (Section 158
Postal Manual) Do Not Return